Fundamental measure theory for hard-sphere mixtures revisited: the White Bear version

2002 J. Phys.: Condens. Matter 14 12063

(http://iopscience.iop.org/0953-8984/14/46/313)

INSTITUTE OF PHYSICS PUBLISHING JOURNAL OF PHYSICS: CONDENSED MATTER

J. Phys.: Condens. Matter **14** (2002) 12063–12078 PII: S0953-8984(02)38426-1

Fundamental measure theory for hard-sphere mixtures revisited: the White Bear version

R Roth[1,2], **R Evans**[3], **A Lang**[4] **and G Kahl**[4]

[1] Max-Planck Institut für Metallforschung, Heisenbergstraße 1, D-70689 Stuttgart, Germany
[2] Institut für Theoretische und Angewandte Physik, Universität Stuttgart, Pfaffenwaldring 57, D-70569 Stuttgart, Germany
[3] University of Bristol, H H Wills Physics Laboratory, Royal Fort, Tyndall Avenue, Bristol BS8 1TL, UK
[4] Institut für Theoretische Physik and CMS, TU Wien, Wiedner Hauptstraße 8-10, A-1040 Wien, Austria

E-mail: Roland.Roth@mf.mpg.de

Received 20 June 2002
Published 8 November 2002
Online at stacks.iop.org/JPhysCM/14/12063

Abstract

We develop a density functional for hard-sphere mixtures which keeps the structure of Rosenfeld's fundamental measure theory (FMT) whilst inputting the Mansoori–Carnahan–Starling–Leland bulk equation of state. Density profiles for the pure hard-sphere fluid and for some binary mixtures adsorbed at a planar hard wall obtained from the present functional exhibit some improvement over those from the original FMT. The pair direct correlation function $c^{(2)}(r)$ of the pure hard-sphere fluid, obtained from functional differentiation, is also improved. When a tensor weight function is incorporated for the pure system our functional yields a good description of fluid–solid coexistence and of the properties of the solid phase.

1. Introduction

In 1989 Rosenfeld [1] introduced novel ideas for deriving a density functional theory (DFT) for hard-sphere mixtures. His approach, which is distinctly different from earlier non-local, weighted density approximations (WDA) [2], is based on the geometrical properties of the spheres and is termed fundamental measure theory (FMT). The original version met with considerable success when applied to a variety of inhomogeneous situations, including the hard-sphere fluid adsorbed at walls and confined in model pores [1, 2]. Although the original version could not describe a stable crystalline phase the FMT was refined [3, 4] in order to incorporate the freezing transition. These refinements and subsequent improvements/modifications of FMT have all focused on the zero-dimensional limit, i.e. the limit which pertains to a narrow cavity that can contain at most one sphere. Requiring the DFT to yield the exact free energy

in the zero-dimensional limit provided new insight into the structure of FMT and suggested new prescriptions for functionals that could describe situations of extreme confinement [3, 4]. More recently Tarazona and Rosenfeld [5–7] have argued that the hard-sphere free-energy functional can be constructed solely from the requirement that the functional reproduces the exact zero-dimensional limit for cavities of different shapes; the equation of state and the correlation functions of the homogeneous fluid are then given as output from, rather than input to, the DFT. This particular strategy is reviewed briefly in [6, 8].

One of the main limitations of the original FMT, and indeed of its successors, is that the underlying bulk fluid equation of state is the Percus–Yevick (PY) compressibility equation, equivalent to scaled particle theory (SPT). As is well known, for the case of the pure hard-sphere fluid this implies that the pressure p is overestimated for fluid densities approaching that at bulk freezing [9]. An important consequence is that ρ_w, the contact value of the density of the pure hard-sphere fluid at a planar wall, is significantly overestimated at high bulk (reservoir) densities. This follows from the wall contact theorem: $\rho_w = \beta p$, where $\beta = 1/k_B T$. The density profiles obtained from FMT obey this theorem, with p referring to the underlying equation of state. Similarly for a ν component mixture of hard spheres at the planar hard wall the contact values ρ_{wi}, for species $i = 1, \ldots, \nu$, should satisfy the generalized contact theorem

$$\sum_i \rho_{wi} = \beta p. \tag{1}$$

A further, potentially more serious, consequence of the inaccuracy of the underlying PY fluid equation of state is that the FMT, suitably modified to include a tensor measure, predicts coexisting fluid and solid densities that are rather low w.r.t. computer simulation results [8].

In the present paper we describe a DFT for hard-sphere mixtures which preserves the basic structure and, hence, much of the elegance of the FMT, while seeking to improve the overall accuracy by replacing the underlying PY compressibility equation of state by the empirical Mansoori–Carnahan–Starling–Leland (MCSL) [10] equation, known to provide a more accurate description of hard-sphere mixtures. Earlier attempts to incorporate the accurate Carnahan–Starling [11] equation of state into DFT for pure hard-sphere fluids were based on either the Tarazona WDA [2, 12] or a generating function approach [13]. Here we retain the weight functions and hence the weighted densities of the original FMT, but modify the ansatz for the free-energy density that enters the functional. Our modification is similar in spirit to that employed by Tarazona [8] in his very recent treatment of the one-component system. We find that our present approach provides a more accurate account of the density profiles, especially near contact, of both pure hard spheres and mixtures adsorbed at a planar hard wall than that provided by the original FMT. It also provides a better account of fluid–solid coexistence. The paper is arranged as follows: in section 2 we describe the original FMT and how this can be modified to incorporate the MCSL equation of state. We also discuss the self-consistency of the approach. Section 3 focuses on the fluid phase properties and we show in section 3.1 that the new functional generates a pair direct correlation function for the pure bulk fluid that is closer to simulation results that the usual PY solution. Results for density profiles at hard walls are presented in section 3.2. Solid phase properties are described in section 4. We conclude with a summary and discussion in section 5.

2. Theory

2.1. Rosenfeld fundamental measure theory

Since what follows is based strongly on Rosenfeld's ideas and the experience gained by applications of the FMT it is useful to recall some known features of the FMT. In order

to construct a density functional for a mixture consisting of ν species of hard spheres, with $\nu \geqslant 1$, Rosenfeld used the exact low density result for the excess (over ideal gas) Helmholtz free-energy functional, valid in the limit where all the one-body densities $\{\rho_i(\boldsymbol{r})\} \to 0$,

$$\beta\mathcal{F}_{ex}[\{\rho_i\}] = -\tfrac{1}{2}\sum_{i,j}\int \mathrm{d}^3r \int \mathrm{d}^3r'\, \rho_i(\boldsymbol{r})\rho_j(\boldsymbol{r}')f_{ij}(|\boldsymbol{r}-\boldsymbol{r}'|) \tag{2}$$

as a starting point. He noted that the Mayer f function, defined by

$$f_{ij}(r) = \exp(-\beta V_{ij}(r)) - 1 \tag{3}$$

where $V_{ij}(r)$ is the pair potential between two species i and j, can be decomposed into the form

$$-f_{ij}(r) = \omega_3^i \otimes \omega_0^j + \omega_0^i \otimes \omega_3^j + \omega_2^i \otimes \omega_1^j + \omega_1^i \otimes_2^j - \vec{\omega}_2^i \otimes \vec{\omega}_1^j - \vec{\omega}_1^i \otimes \vec{\omega}_2^j \tag{4}$$

for a hard-sphere mixture, with the weight functions given by

$$\omega_3^i(\boldsymbol{r}) = \Theta(R_i - r), \tag{5}$$

$$\omega_2^i(\boldsymbol{r}) = \delta(R_i - r), \tag{6}$$

$$\omega_1^i(\boldsymbol{r}) = \frac{\omega_2^i(\boldsymbol{r})}{4\pi R_i}, \tag{7}$$

$$\omega_0^i(\boldsymbol{r}) = \frac{\omega_2^i(\boldsymbol{r})}{4\pi R_i^2}, \tag{8}$$

$$\vec{\omega}_2^i(\boldsymbol{r}) = \frac{\boldsymbol{r}}{r}\delta(R_i - r), \tag{9}$$

$$\vec{\omega}_1^i(\boldsymbol{r}) = \frac{\vec{\omega}_2^i(\boldsymbol{r})}{4\pi R_i}, \tag{10}$$

where $\Theta(r)$ is the Heaviside function and $\delta(r)$ is the Dirac delta function. The symbol $\otimes$ in equation (4) denotes the convolution of the weight functions. It is important to note that the deconvolution, equation (4), would appear to be unnecessarily complicated if only a pure hard-sphere fluid were to be considered. For a mixture, however, this particular structure is suggested by that of the *exact* one-dimensional functional of the mixture of hard rods [14, 15]. It is also interesting to note that an alternative deconvolution of the Mayer f function, suggested by Kierlik and Rosinberg [16], avoids vector-like weight functions but introduces instead weights containing first and second derivatives of the Dirac delta function. Although it was proven later that both choices of weight functions lead to an equivalent functional for the hard-sphere mixture [17], it now appears that Rosenfeld's choice is more general in its scope. In particular, it allows for an approximate generalization to convex non-spherical hard particles [18, 19]. Here we will follow the notation and the choice of weights given in equation (4).

The weight functions give rise to a set of weighted densities $\{n_\alpha(\boldsymbol{r})\}$ for the ν-component mixture. These are defined as

$$n_\alpha(\boldsymbol{r}) = \sum_{i=1}^{\nu}\int \mathrm{d}^3r'\, \rho_i(\boldsymbol{r}-\boldsymbol{r}')\omega_\alpha^i(\boldsymbol{r}'), \tag{11}$$

i.e. the sum of the convolutions of the density profiles of each species with its weight function. α labels the four scalar and two vector weights. In the bulk, where the density profiles reduce to constant bulk densities ρ_{bulk}^i, both vector-like weighted densities $\vec{n}_1$ and $\vec{n}_2$ vanish while the scalar weighted densities reduce to the so-called SPT [20] variables: $n_3 \to \xi_3 = 4\pi\sum_i \rho_{bulk}^i R_i^3/3$, $n_2 \to \xi_2 = 4\pi\sum_i \rho_{bulk}^i R_i^2$, $n_1 \to \xi_1 = \sum_i \rho_{bulk}^i R_i$ and $n_0 \to \xi_0 = \sum_i \rho_{bulk}^i$. Note that ξ_3 then corresponds to the total packing fraction.

As an appropriate ansatz for the excess free-energy functional, Rosenfeld used the low-density limit, $\{\rho_i(\boldsymbol{r})\} \to 0$, equation (2) and dimensional analysis to write the excess free-energy functional in the form

$$\beta\mathcal{F}_{ex}[\{\rho_i\}] = \int \mathrm{d}^3r'\, \Phi(\{n_\alpha(\boldsymbol{r}')\}) \tag{12}$$

with Φ, the reduced free-energy density, a *function* of the weighted densities:

$$\Phi = f_1(n_3)n_0 + f_2(n_3)n_1n_2 + f_3(n_3)\vec{n}_1\cdot\vec{n}_2 + f_4(n_3)n_2^3 + f_5(n_3)n_2\vec{n}_2\cdot\vec{n}_2. \tag{13}$$

Each term in (13) has the dimension of number density, i.e. (length)$^{-3}$. In order to ensure that the ansatz, equations (12) and (13), recovers the deconvolution of the Mayer f function, equation (4), it is necessary to require that to lowest order in n_3 the unknown functions f_1, f_2, f_3 have expansions of the form $f_1 = n_3+\mathcal{O}(n_3^2)$, $f_2 = 1+\mathcal{O}(n_3)$ and $f_3 = -1+\mathcal{O}(n_3)$. Moreover, $f_4 = 1/24\pi + \mathcal{O}(n_3)$, and $f_5 = -3/24\pi + \mathcal{O}(n_3)$.

Although the ansatz in equation (13) is constructed to reproduce *exactly* the low-density limit, it is clear that for intermediate and high densities this ansatz must ensure that the weight functions, and hence the weighted densities, required by the low-density limit are sufficient to approximate the simultaneous interaction of three or more spheres. The functions $f_1, \ldots, f_5$ can be determined by requiring that the resulting functional satisfies a thermodynamic condition. In the original derivation Rosenfeld used the SPT equation [20]

$$\lim_{R_i\to\infty} \frac{\mu_{ex}^i}{V_i} = p, \tag{14}$$

with $V_i = 4\pi R_i^3/3$ the volume of a spherical particle with radius R_i and μ_{ex}^i the excess chemical potential of species i. This relation, which we will discuss in more detail in section 2.3, relates the excess chemical potential for insertion of a big spherical particle with a radius R_i, to the leading-order term pV_i in the reversible work necessary to create a cavity big enough to hold this particle. The pressure entering equation (14) can be determined self-consistently in terms of the weighted densities from equation (13). The solution found by Rosenfeld [1] and denoted RF is

$$f_1^{RF}(n_3) = -\ln(1-n_3), \tag{15}$$

$$f_2^{RF}(n_3) = \frac{1}{1-n_3}, \tag{16}$$

$$f_3^{RF}(n_3) = -f_2^{RF}(n_3), \tag{17}$$

$$f_4^{RF}(n_3) = \frac{1}{24\pi(1-n_3)^2}, \tag{18}$$

$$f_5^{RF}(n_3) = -3f_4^{RF}(n_3), \tag{19}$$

and it is straightforward to see that these solutions satisfy the aforementioned conditions for the low-density limit. It is worthwhile to note that the conditions $f_3 = -f_2$ and $f_5 = -3f_4$, that fix the dependence of the functional on the vector weighted densities $\vec{n}_1$ and $\vec{n}_2$, follow from equation (14) only if it is assumed that the SPT differential equation, which is by construction a bulk equation, remains valid for slightly inhomogeneous situations. Since the vector weighted densities vanish in the bulk limit it is, strictly speaking, impossible to determine the functions f_3 and f_5 from bulk thermodynamics alone. Given the success of the Rosenfeld functional in various applications we choose to retain the conditions (17) and (19) in the subsequent modifications.

The resulting functional, that we refer to as the original Rosenfeld (RF) functional, is usually written in the form $\Phi = \Phi_1 + \Phi_2 + \Phi_3$ with

$$\Phi_1^{RF} = -n_0 \ln(1 - n_3), \tag{20}$$

$$\Phi_2^{RF} = \frac{n_1 n_2 - \vec{n}_1 \cdot \vec{n}_2}{1 - n_3}, \tag{21}$$

$$\Phi_3^{RF} = \frac{n_2^3 - 3n_2 \vec{n}_2 \cdot \vec{n}_2}{24\pi(1 - n_3)^2}. \tag{22}$$

Although this functional was found to be very successful and often very accurate in accounting for various properties of highly inhomogeneous fluid phases, it failed to predict the fluid to solid phase transition of the pure hard-sphere system. This failing was first remedied empirically by Rosenfeld *et al* [3, 4] who modified the dependence of Φ_3 on the weighted densities n_2 and $\vec{n}_2$, taking into account certain features of 'dimensional crossover'. The modifications were found to perform better than the original Rosenfeld DFT for densely packed fluids in spherical cavities—a situation of extreme confinement [21, 22]

Subsequently Tarazona and Rosenfeld [5–7] derived an FMT especially designed to study the properties of the one-component hard-sphere solid. They began with the so-called zero-dimensional limit which considers a narrow cavity that can hold at most a single sphere. Starting with the free-energy function for this narrow pore, functionals are derived for higher embedding dimensions. A three-dimensional functional based on this idea reproduces the original Rosenfeld functional. In [7] it is pointed out, however, that there are shapes of zero-dimensional cavities which cannot be described by the particular set of weight functions chosen in the original FMT. The problem becomes more acute with increasing embedding dimension. In order to remedy this defect, Tarazona [7] introduced a new second-rank tensor-like weight function $\omega_{m_2}(\boldsymbol{r})$ and adapted the contribution Φ_3 to the functional. In the notation introduced in [23], we write the tensor weight function as

$$\omega_{m_2}(\boldsymbol{r}) = \omega_2(\boldsymbol{r})(\boldsymbol{r}\boldsymbol{r}/r^2 - \hat{1}/3), \tag{23}$$

with $\hat{1}$ denoting the unit matrix. This gives rise to a new tensor weighted density n_{m_2}. The new Φ_3^T term of the Tarazona FMT is given by [7, 23]

$$\Phi_3^T = \frac{1}{24\pi(1 - n_3)^2}(n_2^3 - 3n_2 \vec{n}_2 \cdot \vec{n}_2 + 9(\vec{n}_2 n_{m_2} \vec{n}_2 - \mathrm{Tr}(n_{m_2}^3)/2)), \tag{24}$$

and the application of the augmented functional to the hard-sphere solid provided an excellent account of simulation results for the equation of state and for other properties of the solid. The extension of this approach to hard-sphere mixtures requires the introduction of a new third-rank tensor-like weight function [24].

2.2. Derivation of the new functional

Building upon the ideas presented so far, we are now ready to construct a new functional. We retain the same weight functions and the same form (12) for the functional but use a different thermodynamic condition in order to specify the coefficients $f_1, \ldots, f_5$ of the ansatz (13). In contrast to existing FMT functionals which output the equation of state (for fluid states this is the PY compressibility equation), we use the MCSL equation of state [10], which is a generalization to the ν-component hard-sphere fluid of the accurate, one-component Carnahan–Starling equation of state [11], as an *input*. We prescribe the functions $f_1, \ldots, f_5$, retaining the two conditions (17) and (19), such that the equation of state which underlies the new functional is the MCSL pressure. For this approach to be feasible it is important that the MCSL equation

of state is based on the same SPT variables $\xi_0, \ldots, \xi_3$ which enter the PY compressibility equation of state underlying the original FMT. The MCSL pressure is given by

$$\beta p_{MCSL} = \frac{n_0}{1-n_3} + \frac{n_1 n_2}{(1-n_3)^2} + \frac{n_2^3}{12\pi(1-n_3)^3} - \frac{n_3 n_2^3}{36\pi(1-n_3)^3}, \tag{25}$$

where $\{n_\alpha\} \equiv \{\xi_\alpha\}$ for the bulk fluid. The final term in (25) is absent in the PY result.

Incorporating the deconvolution of the Mayer f function and imposing the conditions (17) and (19), we employ an ansatz for Φ of the form

$$\Phi = f_1(n_3)n_0 + f_2(n_3)(n_1 n_2 - \vec{n}_1 \cdot \vec{n}_2) + f_4(n_3)(n_2^3 - 3n_2 \vec{n}_2 \cdot \vec{n}_2). \tag{26}$$

In order to determine the three unknown functions f_1, f_2, and f_4 we note that the pressure and the grand potential Ω_{bulk} of a bulk mixture are related by

$$\Omega_{bulk} = -pV, \tag{27}$$

where V is the total volume, $\Omega_{bulk} = (\beta^{-1}\Phi_{bulk} + f^{id}_{bulk} - \sum_i \mu_i \rho_i)V$, $f^{id}_{bulk} = \beta^{-1}\sum_i \rho^i_{bulk}(\ln \lambda_i^3 \rho^i_{bulk} - 1)$ is the ideal gas free-energy density and $\mu_i = \partial(\beta^{-1}\Phi_{bulk} + f^{id}_{bulk})/\partial\rho^i_{bulk}$ is the chemical potential of species i. Equation (27) requires that the pressure should satisfy the equation

$$-\beta p = \Phi_{bulk} - \sum_{\alpha=0}^{3} \frac{\partial \Phi_{bulk}}{\partial n_\alpha} n_\alpha - n_0, \tag{28}$$

with the sum over the scalar weighted densities only; recall that $\{n_\alpha\} \equiv \{\xi_\alpha\}$ for the bulk fluid. Substituting (25) and (26) into (28) we obtain a differential equation which can be solved easily and we find $f_1(n_3) = f_1^{RF}(n_3)$, $f_2(n_3) = f_2^{RF}$ and

$$f_4(n_3) = \frac{n_3 + (1-n_3)^2 \ln(1-n_3)}{36\pi n_3^2 (1-n_3)^2}. \tag{29}$$

The resulting excess free-energy function is given by

$$\Phi = -n_0 \ln(1-n_3) + \frac{n_1 n_2 - \vec{n}_1 \cdot \vec{n}_2}{1-n_3} + (n_2^3 - 3n_2 \vec{n}_2 \cdot \vec{n}_2)\frac{n_3 + (1-n_3)^2 \ln(1-n_3)}{36\pi n_3^2 (1-n_3)^2} \tag{30}$$

which should be compared with the original Rosenfeld form, equations (20)–(22). Note that in the low-density limit we obtain $\lim_{n_3 \to 0} f_4(n_3) = 1/(24\pi)$, i.e. the same value as from the original Rosenfeld functional (see equation (22)). Thus we are guaranteed to recover the exact low-density limit.

As the derivation of the new functional has followed that of the original Rosenfeld FMT very closely, it faces similar problems when it is applied to the freezing transition. However, the same procedures that remedied the failings for the original FMT can be used for the new functional. Thus, it is possible to follow the empirical procedure of [3, 4] and modify the dependence of Φ_3 on the weighted densities n_2 and $\vec{n}_2$ in the new functional. This approach would enable the functional to treat a hard-sphere mixture. Equally well it is possible to follow Tarazona [7] who introduced a tensor-like weighted density in order to study the properties of the *one-component* hard-sphere solid. This is the route we employ here, i.e. in the present calculations for the solid phase we replace the term $(n_2^3 - 3n_2\vec{n}_2 \cdot \vec{n}_2)$ in equation (30) by the numerator of Tarazona's expression (24) so that the present Φ_3 is given by

$$\Phi_3 = \frac{n_3 + (1-n_3)^2 \ln(1-n_3)}{36\pi n_3^2 (1-n_3)^2}(n_2^3 - 3n_2 \vec{n}_2 \cdot \vec{n}_2 + 9(\vec{n}_2 n_{m_2} \vec{n}_2 - \mathrm{Tr}(n^3_{m_2})/2)). \tag{31}$$

2.3. Test for self-consistency

As mentioned in section 2.1, Rosenfeld [1] used the scaled particle equation (14) to determine the functions $f_1, \ldots, f_5$. Here we re-examine this equation in the context of self-consistency for the functional.

First we note that the excess chemical potential of inserting a single big hard sphere of species i and radius R_i into a fluid of hard spheres is the reversible work done to create a cavity that is large enough to hold this inserted hard sphere. In SPT one starts with a pointlike cavity and increases its size until it is sufficiently large. Clearly, when increasing the cavity size one must work against the pressure of the fluid resulting in a term pV_i, where $V_i = 4\pi R_i^3/3$. Since the surface area of the sphere is also increased, work must also be done against the surface tension. This second term is proportional to the surface area $A_i = 4\pi R_i^2$. Moreover for finite values of R_i the surface tension will also depend on the radius of curvature so there will be an additional term that is proportional to R_i. If, however, we divide the excess chemical potential by the volume V_i it is easy to see that equation (14) follows and that it is exact in the limit $R_i \to \infty$.

The connection to FMT can be made by noting that the excess chemical potential takes the form

$$\beta\mu_i^{ex} = \sum_{\alpha=0}^{3} \frac{\partial\Phi_{bulk}}{\partial n_\alpha}\frac{\partial n_\alpha}{\partial\rho_{bulk}^i} \tag{32}$$

$$= \frac{\partial\Phi_{bulk}}{\partial n_3}V_i + \frac{\partial\Phi_{bulk}}{\partial n_2}A_i + \frac{\partial\Phi_{bulk}}{\partial n_1}R_i + \frac{\partial\Phi_{bulk}}{\partial n_0}, \tag{33}$$

and we used the definition of the SPT variables $n_\alpha \equiv \xi_\alpha$ given earlier. Equation (33) has precisely the same form as the SPT expansion so it is clear that for any FMT functional the coefficient of the leading volume term should be identified with βp, i.e. the relation

$$\frac{\partial\Phi_{bulk}}{\partial n_3} = \beta p \tag{34}$$

should be obeyed.

In the derivation of the original Rosenfeld functional equation (34) is *imposed*, i.e. the left-hand side of equation (28) is identified with $-\partial\Phi_{bulk}/\partial n_3$ and the resulting SPT differential equation is solved. The pressure which results is the SPT or, equivalently, the PY compressibility equation of state. For the present functional, however, equation (34) is *not* imposed and we find from equation (30) that

$$\frac{\partial\Phi}{\partial n_3} = \frac{n_0}{1-n_3} + \frac{n_1 n_2}{(1-n_3)^2} - \frac{n_2^3(2+n_3(n_3-5))}{36\pi n_3^2(1-n_3)^3} - \frac{n_2^3\ln(1-n_3)}{18\pi n_3^3}, \tag{35}$$

which evidently is different from the MCSL equation of state (25). The difference arising from this inconsistency was examined within the context of the one-component fluid where the pressure input into the theory is the accurate Carnahan–Starling equation of state, p_{CS}. We show both the Carnahan–Starling equation of state (solid curve) and the pressure obtained from equation (35) (dashed curve) in figure 1. The deviation between these two curves is at most 2%. In contrast, the PY compressibility equation of state p_{PY}^c, also shown in figure 1 (dotted curve), overestimates the pressure of a hard-sphere fluid close to freezing by up to 7%.

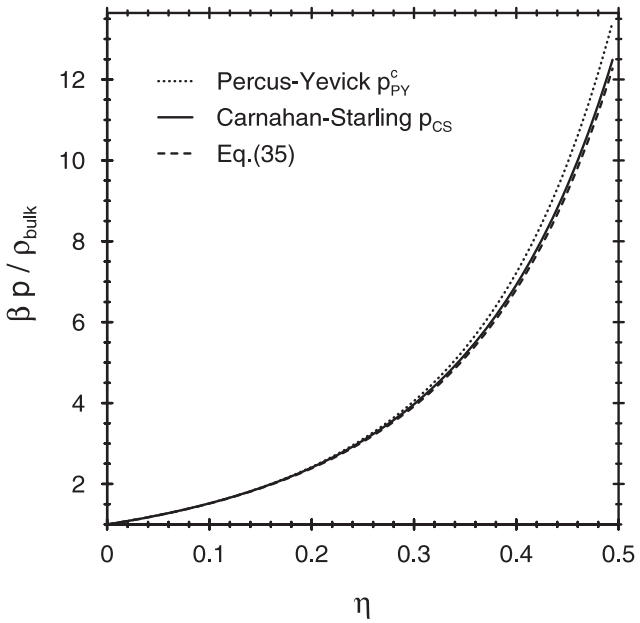

Figure 1. The equation of state of the pure hard-sphere fluid versus packing fraction η. For the present DFT the Carnahan–Starling pressure is imposed by the theory. The pressure given by $\beta^{-1}\partial\Phi/\partial n_3$ in equation (35) deviates very slightly from Carnahan–Starling, attesting to the high degree of self-consistency of the approach.

3. Fluid phase properties

3.1. Pair direct correlation function $c^{(2)}(r)$

In this section we employ the new functional (30) to derive the direct pair correlation functions $c^{(2)}_{ij}(r)$ for a bulk fluid mixture. These are defined within DFT as

$$c^{(2)}_{ij}(|\boldsymbol{r}-\boldsymbol{r}'|) = -\left.\frac{\delta^2\beta\mathcal{F}_{ex}}{\delta\rho_i(\boldsymbol{r})\delta\rho_j(\boldsymbol{r}')}\right|_{\rho_i(\boldsymbol{r})=\rho^i_{bulk},\rho_j(\boldsymbol{r}')=\rho^j_{bulk}} \tag{36}$$

and can be calculated from an FMT functional such as the original Rosenfeld functional or (30) via

$$c^{(2)}_{ij}(r) = -\sum_{\alpha,\beta}\frac{\partial^2\Phi}{\partial n_\alpha\partial n_\beta}\omega^i_\alpha\otimes\omega^j_\beta. \tag{37}$$

For the Rosenfeld functional equation (37) generates the well known PY pair direct correlation functions $c^{(2),PY}_{ij}(r)$, which are polynomials of third order in r for $r \leqslant R_i + R_j$ and which vanish identically for $r > R_i + R_j$. Since we employ the same weight functions as Rosenfeld, it is clear that the new functional will also generate direct correlation functions which vanish for $r > R_i + R_j$. Moreover we know that for small densities the present functional reduces to that of Rosenfeld suggesting that the direct correlation functions should reduce to the PY result in the same limit.

Following the notation of [1] we introduce the functions

$$\chi^{(\alpha)} = \frac{\partial^2\Phi}{\partial n_\alpha\partial n_3} \tag{38}$$

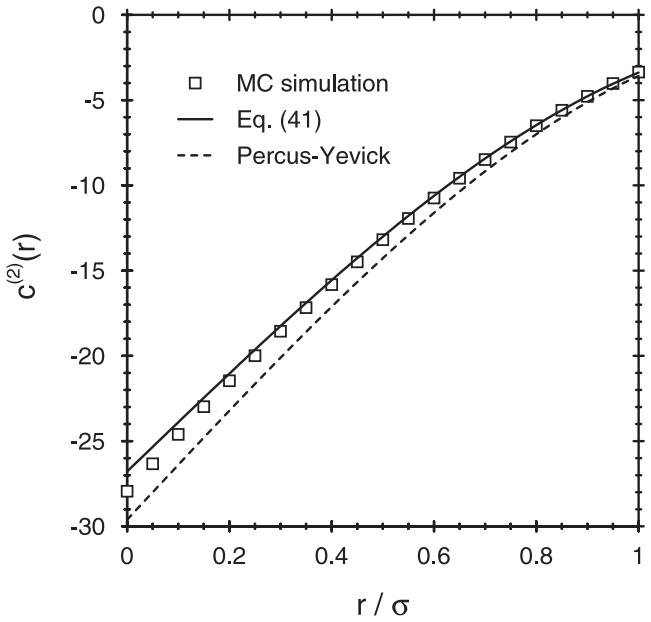

Figure 2. Comparison between MC simulation data [25] for the pair direct correlation function of a pure hard-sphere fluid $c^{(2)}(r)$ (symbols), the present theory (full curve) and PY theory (dashed curve) for packing fraction $\eta = 0.8\pi/6 \approx 0.4189$. Both the present and PY theories yield $c^{(2)}(r) = 0$ for $r > 2\sigma$ whereas simulations give a rapidly decaying positive tail in this region.

for $\alpha = 0, \ldots, 3$. Given the new form of Φ_3 we must introduce the additional function

$$\chi^{(22)} = \frac{\partial^2 \Phi}{\partial n_2 \partial n_2}. \tag{39}$$

Then we rewrite equation (37) as

$$\begin{aligned} -c_{ij}^{(2)}(r) = {} & \chi^{(3)}(\omega_3^i \otimes \omega_3^j) + \chi^{(2)}(\omega_3^i \otimes \omega_2^j + \omega_2^i \otimes \omega_3^j) \\ & + \chi^{(1)}(\omega_3^i \otimes \omega_1^j + \omega_1^i \otimes \omega_3^j) + \chi^{(22)}(\omega_2^i \otimes \omega_2^j - \vec{\omega}_2^i \otimes \vec{\omega}_2^j) \\ & + \chi^{(0)}(\omega_3^i \otimes \omega_0^j + \omega_0^i \otimes \omega_3^j + \omega_2^i \otimes \omega_1^j + \omega_1^i \otimes \omega_2^j - \vec{\omega}_2^i \otimes \vec{\omega}_1^j - \vec{\omega}_1^i \otimes \vec{\omega}_2^j), \end{aligned} \tag{40}$$

which should be compared with the corresponding result in [1]. For the one-component bulk fluid equation (40) simplifies considerably and the resulting direct correlation function, like the PY direct pair correlation function, is a polynomial of third order in r. However, the coefficients are different:

$$\begin{aligned} c^{(2)}(r) = {} & -\frac{1 + \eta(4 + \eta(3 - 2\eta))}{(1-\eta)^4} + \left(\frac{2 - \eta + 14\eta^2 - 6\eta^3}{(1-\eta)^4} + \frac{2\ln(1-\eta)}{\eta} \right) \frac{r}{\sigma} \\ & - \left(\frac{3 + 5\eta(\eta - 2)(1-\eta)}{(1-\eta)^4} + \frac{3\ln(1-\eta)}{\eta} \right) \left(\frac{r}{\sigma} \right)^3, \qquad r \leqslant \sigma, \end{aligned} \tag{41}$$

and $c^{(2)}(r) = 0$ for $r > \sigma$. Here $\sigma = 2R$ is the hard-sphere diameter. Equation (41) reduces to the PY result at first order in η. For $\eta > 0$, equation (41) predicts a value of $c^{(2)}(r = 0)$ which is always less negative than the corresponding PY result. At $r = \sigma$ both theories yield very similar results. Generally the agreement between equation (41) and the simulation results

of [25] is improved with respect to the PY results. An example is shown in figure 2 where we compare $c^{(2)}(r)$ for a pure hard-sphere fluid obtained from the present theory (full curve), equation (41), with that obtained by PY theory (dashed curve) [9] and with the simulation data of [25] for $\eta = 0.8\pi/6 \approx 0.4189$. Note that in PY theory and in the present treatment $c^{(2)}(r)$ is negative for $r \leqslant \sigma$ and is identically zero for $r > \sigma$, while the pair direct correlation function obtained in the simulation has a fast decaying positive tail for $r > \sigma$.

3.2. Hard-sphere fluid at a planar hard wall

A direct test for the new functional in an inhomogeneous situation is the calculation of the density profile of a hard-sphere fluid close to a planar hard wall. The system is characterized by the external potentials

$$V_i(z) = \begin{cases} \infty & \text{for } z < R_i \\ 0 & \text{otherwise.} \end{cases} \tag{42}$$

In this section we examine the accuracy of the present functional for a pure hard-sphere fluid and for a binary mixture of hard spheres close to a planar hard wall by comparing density profiles calculated by minimizing the grand potential functional

$$\Omega[\{\rho_i\}] = \mathcal{F}_{ex}[\{\rho_i\}] + \int \mathrm{d}^3 r \; f^{id}(\{\rho_i\}) + \sum_{i=1}^{\nu} \int \mathrm{d}^3 r \; \rho_i(z)(V_i(z) - \mu_i) \tag{43}$$

with those from simulation.

We begin by calculating density profiles of a pure hard-sphere fluid at a planar hard wall for various packing fractions $\eta = \pi \rho_{bulk} \sigma^3/6$ of the bulk fluid far from the wall. For all values of η in the liquid phase, i.e. $\eta < \eta^f = 0.494$, we find that the overall agreement between the results of the present DFT and those of the original Rosenfeld functional is very good. Furthermore we find that both the present theory and the original Rosenfeld functional yield density profiles which agree very well with MC simulation results from [26]. One example of the level of agreement between the different approaches, for $\eta = 0.4257$, is shown in figure 3.

Only very close to the wall—see the inset of figure 3—is there a small difference between the results of original Rosenfeld functional and those of the present theory. The reason for this small difference lies in the difference between the underlying equations of state. It was shown in [27, 28] that density functional theories based on a WDA should satisfy the wall contact theorem for planar hard walls, equation (1). For a pure hard-sphere fluid treated by the Rosenfeld functional the pressure is given by the PY compressibility equation of state p^c_{PY} which, for high packing fractions, is significantly too high compared to simulations (see figure 1). The present DFT is constructed in such a way that the underlying equation of state is given by that of MCSL, which in the case of a pure fluid reduces to the well known Carnahan–Starling equation of state p_{CS}. Recall that the latter is found to be in good agreement with simulations and predicts a pressure which is smaller than that given by p^c_{PY} (see figure 1).

Thus for small distances from the wall the density profiles calculated from the present DFT should be closer to simulation than the density profiles obtained from the Rosenfeld functional, as is illustrated in the inset of figure 3. For this particular value of η the difference between p^c_{PY} and p_{CS} is about 5%. It follows that the same difference is also found between the contact values of the density profiles obtained by the Rosenfeld functional and by the present DFT. Note that we have checked numerically that the contact theorem is satisfied for both functionals.

As a second application we focus on a binary hard-sphere mixture. We have calculated the density profiles of both components for various values of the packing fraction of the small

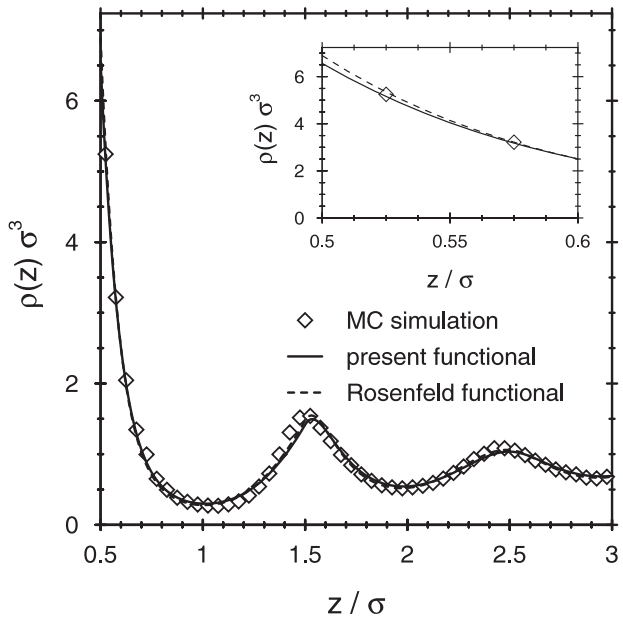

Figure 3. Density profile of a one-component hard-sphere fluid at a planar hard wall for $\eta = 0.4257$. The full curve denotes the density profile of the present theory, the dashed curve that of the original Rosenfeld functional and the symbols denote results obtained from simulation [26]. The results from the two DFTs lie almost on top of each other except for values of z very close to contact (see inset).

spheres, η_s, and that of the big spheres, η_b, and various size ratios $q = \sigma_s/\sigma_b$ and compared results with simulation data from [29] and with results obtained using the original Rosenfeld functional [30]. As was the case for the pure fluid, we observe good overall agreement between the various approaches. In figure 4 we show a comparison for the density profile of the small spheres (a) and that of the big spheres (b) of a binary hard-sphere mixture with $\eta_s = 0.0047$, $\eta_b = 0.3859$ and $q = \sigma_s/\sigma_b = 1/3$. Once again we find that the only significant deviation between results obtained from the present DFT and those from the Rosenfeld functional are for values of z very close to the wall. This is illustrated in the inset to figure 4(b).

Both DFTs satisfy the contact theorem, equation (1). For the present functional the sum of the contact densities equals βp_{MCSL}, while for the original functional the sum is equal to βp^c_{PY}, the scaled particle result. It is important to emphasize that the sum rule (1) does not allow us to make statements about the contact densities $\rho_{wi} \equiv \rho_i(R_i^+)$ of individual species; it pertains to the *total* density.

The results for the density profiles shown in figures 3 and 4 were obtained without tensor contributions to the DFT, i.e. we take $n_{m_2} \equiv 0$. Including the tensor contribution, see equation (31), for the one-component case yields almost identical results.

4. Solid phase properties

Having shown that the present functional treats both the bulk and the inhomogeneous fluid phase accurately, we now study some properties of the one-component hard-sphere (bulk) solid. To this end we parametrize the density profile of the solid using the usual Gaussian form

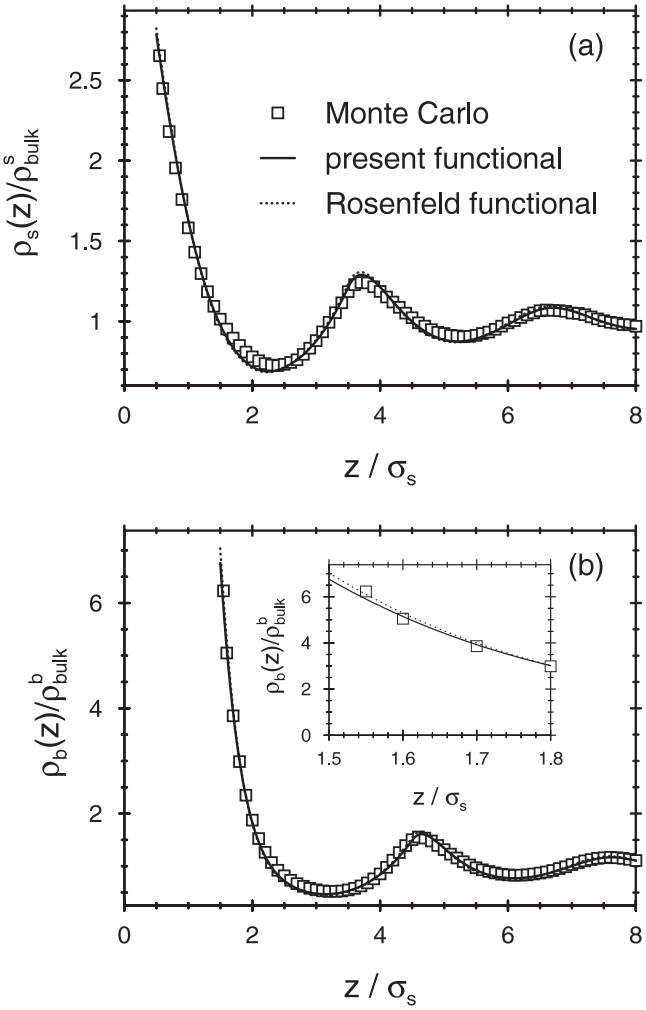

Figure 4. Density profiles of the small spheres (a) and the big spheres (b) of a binary hard-sphere mixture with diameters $\sigma_b = 3\sigma_s$, $\eta_s = 0.0047$ and $\eta_b = 0.3859$. The symbols, full curve and dotted curve denote simulation data from [29], results obtained from the present theory and the Rosenfeld functional, respectively. The results from the two DFTs lie almost on top of each other except for values of z very close to contact—see inset to (b). Note that contact occurs at $z = \sigma_s/2$ for $\rho_s(z)$ and at $z = 3\sigma_s/2$ for $\rho_b(z)$.

$$\rho(\boldsymbol{r}) = \left(\frac{\alpha}{\pi}\right)^{\frac{3}{2}} \sum_{\{\boldsymbol{R}\}} \mathrm{e}^{-\alpha(\boldsymbol{r}-\boldsymbol{R})^2}, \tag{44}$$

where the parameter $\alpha^{-1/2}$ is proportional to the mean width of a peak and the sum is taken over lattice points $\{\boldsymbol{R}\}$ of an fcc lattice. Inputting the density profile, equation (44), into the tensor version of the present functional (see equation (31)) and minimizing the grand potential functional (with $V_i \equiv 0$) with respect to both the lattice size and the Gaussian parameter α, we can determine the equilibrium densities of the hard-sphere fluid and solid at phase coexistence as well as properties of the hard-sphere solid. We find that a hard-sphere fluid of density $\rho^f\sigma^3 = 0.934$ (which corresponds to a packing fraction of $\eta^f = 0.489$) coexists with a

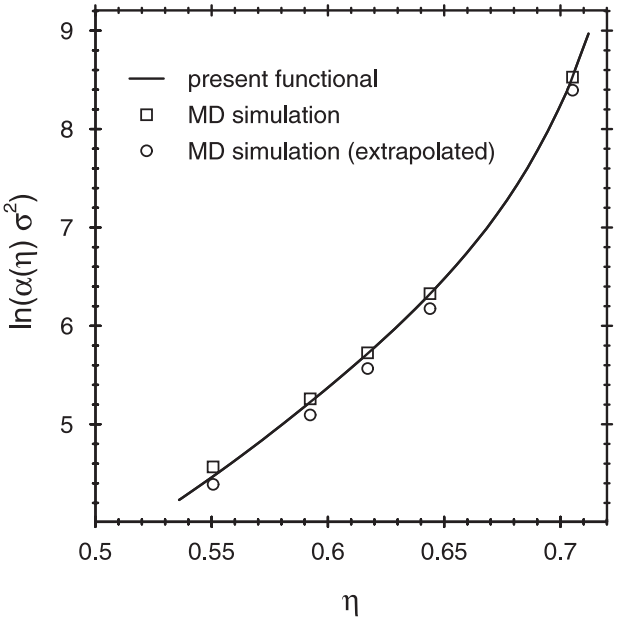

Figure 5. The logarithm of the Gaussian parameter $\alpha(\eta)$ for the fcc solid as a function of the packing fraction η. The solid curve obtained from the minimization of the present functional using the parametrized density profile, equation (44), is compared to MD results [32] for $N = 500$ particles (squares) and extrapolated to $N \to \infty$ (circles).

solid of density $\rho^s\sigma^3 = 1.023$ (corresponding to $\eta^s = 0.536$). These values are in perfect agreement with those found by Tarazona in [8], who also introduced a modification that yields the Carnahan–Starling equation of state for the fluid, and are very close to the coexisting densities found in computer simulations: $\rho^f_{sim}\sigma^3 = 0.940$ and $\rho^s_{sim}\sigma^3 = 1.040$ [31]. The results for the coexisting densities take on additional significance when one considers that the corresponding results obtained from Tarazona's tensor weight DFT [7], which does not have any Carnahan–Starling modification, are $\rho^f\sigma^3 = 0.892$ and $\rho^s\sigma^3 = 0.985$. These values were reported in [8] and agree with the results of our own calculations for the same functional. Incorporating the accurate Carnahan–Starling fluid equation of state does seem to improve the description of fluid–solid coexistence.

The Gaussian parameter $\alpha(\eta)$ follows directly from the minimization of the functional and results are shown in figure 5 (solid curve). We compare the DFT results with the molecular dynamics (MD) simulation data of [32]. The squares in figure 5 denote results with $N = 500$ particles and the agreement between these and the DFT results is very good. In [32] Young and Alder also extrapolated their results to the limit $N \to \infty$ and we show these data as circles in figure 5. Although the simulation data exhibit some statistical error and the extrapolation to $N \to \infty$ can be problematical, the good overall level of agreement between our DFT results and those of simulation is very encouraging.

Similar excellent agreement between DFT and MD results is found for the equation of state of the solid. In figure 6 we show a comparison between the present results (solid curve) and the simulation data of [33].

The results in figures 5 and 6 should be compared with those in figures 1 and 2 of [7] where Tarazona presents the corresponding quantities obtained from his tensor weight DFT, i.e. using equation (24). We find that the two functionals yield almost identical solid state properties.

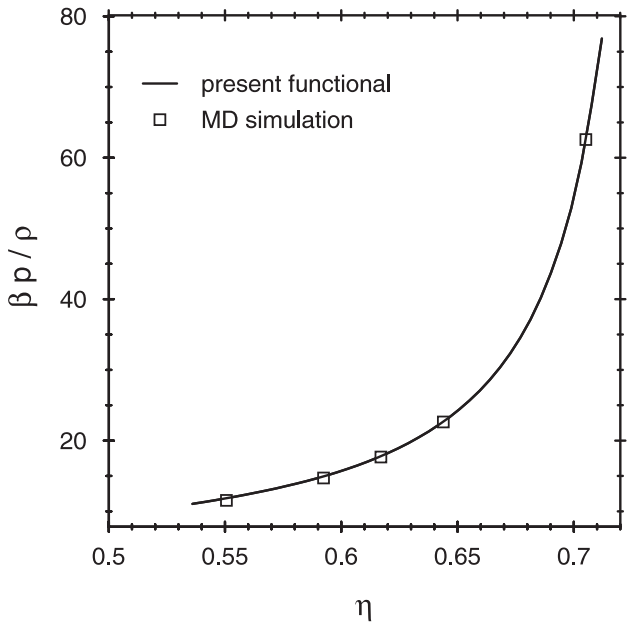

Figure 6. The equation of state $\beta p/\rho$ in the hard-sphere fcc solid as a function of the packing fraction η. The solid curve denotes the present DFT results, and the symbols denote MD results for 500 particles [33].

5. Concluding remarks

We have modified Rosenfeld's original derivation of FMT to obtain a new Helmholtz free-energy functional which has an underlying bulk equation of state equal to that of MCSL, known to be accurate for hard-sphere mixtures. The resulting functional performs somewhat better than the original in describing the density profiles of a pure hard-sphere fluid and of binary mixtures adsorbed at a planar hard wall. In particular, the densities close to contact are given more accurately when the bulk (reservoir) densities are high (figures 3 and 4). By incorporating a tensor-like weight function of the type introduced by Tarazona [7], we find that the present approach provides a good account of fluid–solid coexistence for pure hard spheres. It also yields results for the equation of state and the Gaussian parameter α of the pure solid phase that are of a similar quality to those of [7], although we have not made a detailed examination of properties in the close-packing limit $\eta \to \eta_{cp} = \pi\sqrt{2}/6 = 0.7405$, where the Tarazona prescription is essentially exact. Nor have we investigated the metastable bcc lattice [7].

It is likely that our present approach will prove most useful for treating hard-sphere mixtures adsorbed at walls or confined in pores. Indeed the functional has already been applied to a pure hard-sphere fluid near a hard 90° wedge. The results for density profiles are in significantly better agreement with MC simulations than those from the original Rosenfeld FMT [34]. The present functional should also have advantages over the original FMT when applied to the calculation of liquid radial distribution functions $g_{ij}(r)$ via the test particle route.

Of course the underlying MCSL equation of state will itself become inaccurate for extreme size ratios $q = \sigma_s/\sigma_b \ll 1$ but one could expect a theory based on MCSL to be generally more reliable than one based on the PY equation of state.

We conclude by returning to issues of self-consistency. As emphasized in section 2.3, whilst our present functional does not satisfy equation (34) exactly the degree of inconsistency

is 2% or less at the highest fluid phase densities of pure hard spheres. It would be interesting to perform a similar test for the case of mixtures. Although the pair direct correlation function $c^{(2)}(r)$ obtained by functional differentiation is closer to simulation inside the hard core $r < \sigma$ than the PY result (figure 2), there is no reason to expect $g(r)$ obtained from this $c^{(2)}(r)$ via the Ornstein–Zernike equation to satisfy the core condition $g(r) \equiv 0$, $r < \sigma$. However, for the range of state points we have investigated we find that the core condition is only weakly violated. Since the present functional employs the same weight functions as the original Rosenfeld version it cannot account for the decaying tail of $c^{(2)}(r)$ in the region $r > \sigma$. Incorporating such a tail within FMT requires multi-centre convolutions [8].

We have not investigated the higher-body direct correlation functions $c^{(m)}$, $m > 2$, resulting from our present functional but we do not expect those to be qualitatively different from those generated by the original Rosenfeld functional [1].

By basing our functional on the (empirical) MCSL equation of state we have deliberately adopted a more pragmatic approach to fundamental measure treatments of DFT than those which begin with the zero-dimensional limit [5–7]. Since there is nothing sacrosanct about the latter we believe that there is still scope for some diversity of approach!

Acknowledgments

It is a pleasure to thank M Schmidt, J M Brader, Y Rosenfeld, P Tarazona and P Bryk for stimulating discussions. Yasha Rosenfeld's scholorship and personality greatly influenced the authors' views on DFT. We are grateful for the insight he shared with us. AL and GK acknowledge financial support from the Österreichische Forschungsfonds under project nos P13062-TPH and P15857-TPH. AL thanks C N Likos and H Löwen for many helpful discussions and for their kind hospitality at their institute in Düsseldorf. Finally RR and RE would like to thank the staff of the White Bear, St Michael's Hill, Bristol, UK, for providing a congenial and inspiring working environment. Without their technical support the ideas presented here would not have come to fruition.

References

[1] Rosenfeld Y 1989 *Phys. Rev. Lett.* **63** 980
See also
Rosenfeld Y, Levesque D and Weis J-J 1990 *J. Chem. Phys.* **92** 6818
[2] See, e.g.,
Evans R 1992 *Fundamentals of Inhomogeneous Fluids* ed D Henderson (New York: Dekker) p 85
[3] Rosenfeld Y, Schmidt M, Löwen H and Tarazona P 1996 *Phys. Rev.* E **55** 4245
[4] Rosenfeld Y, Schmidt M, Löwen H and Tarazona P 1996 *J. Phys.: Condens. Matter* **8** L577
[5] Tarazona P and Rosenfeld Y 1997 *Phys. Rev.* E **55** R4873
[6] Tarazona P and Rosenfeld Y 1999 *New Approaches to Problems in Liquid State Theory* ed C Caccamoet *et al* (Dordrecht: Kluwer) p 293
[7] Tarazona P 2000 *Phys. Rev. Lett.* **84** 694
[8] Tarazona P 2002 *Physica* A **306** 243
[9] See, e.g.,
Hansen J P and McDonald I R 1986 *Theory of Simple Liquids* (London: Academic)
[10] Mansoori G A, Carnahan N F, Starling K E and Leland T W Jr 1971 *J. Chem. Phys.* **54** 1523
[11] Carnahan N F and Starling K E 1969 *J. Chem. Phys.* **51** 635
[12] Tarazona P 1985 *Phys. Rev.* A **31** 2672
[13] Gonzalez A, White J A and Evans R 1997 *J. Phys.: Condens. Matter* **9** 2375
[14] Percus J K 1976 *J. Stat. Phys.* **15** 505
[15] Vanderlick T K, Davis H T and Percus J K 1989 *J. Chem. Phys.* **91** 7136
[16] Kierlik E and Rosinberg M L 1990 *Phys. Rev.* A **42** 3382

[17] Phan S, Kierlik E, Rosinberg M L, Bildstein B and Kahl G 1993 *Phys. Rev.* E **48** 618
[18] Rosenfeld Y 1994 *Phys. Rev.* E **50** R3318
[19] Rosenfeld Y 1995 *Mol. Phys.* **86** 637
[20] Reiss H, Frisch H L, Helfand E and Lebowitz J L 1960 *J. Chem. Phys.* **32** 119
[21] González A, White J A, Román F L, Velasco S and Evans R 1997 *Phys. Rev. Lett.* **79** 2466
[22] González A, White J A, Román F L and Evans R 1998 *J. Chem. Phys.* **109** 3637
[23] Schmidt M, Löwen H, Brader J M and Evans R 2000 *Phys. Rev. Lett.* **85** 1934
[24] Cuesta J A, Martinez-Raton Y and Tarazona P 2002 *Preprint* cond-mat/0205256
[25] Groot R D, van der Eerden J P and Faber N M 1987 *J. Chem. Phys.* **87** 2263
[26] Groot R D, Faber N M and van der Eerden J P 1987 *Mol. Phys.* **62** 861
[27] van Swol F and Henderson J R 1987 *Phys. Rev.* A **40** 2567
[28] Tarazona P and Evans R 1984 *Mol. Phys.* **52** 847
[29] Noworyta J P, Henderson D, Sokołowski D and Chan K-Y 1998 *Mol. Phys.* **95** 415
[30] Roth R and Dietrich S 2000 *Phys. Rev.* E **62** 6926
[31] Hoover W G and Ree F H 1968 *J. Chem. Phys.* **49** 3609
[32] Young D A and Alder J 1974 *J. Chem. Phys.* **60** 1254
[33] Alder B J, Hoover W G and Young D A 1968 *J. Chem. Phys.* **49** 3688
[34] Bryk P 2002 private communication